# A HEAVY ION POST-ACCELERATOR WITH COUPLED SPIRAL AND SPLIT-RING RESONATORS*

A. Schempp, H. Klein, W. Rohrbach, W. Caspar, G. Lotterbach, E. Müller
Institut für Angewandte Physik, Universität Frankfurt/Main
D-6000 Frankfurt/Main, Germany

## Summary

At the single-ended 7-MV Van de Graff machine in Frankfurt, a small post-accelerator is being built, which will be partly used as a test facility for new linac structures. Therefore different types of resonators will be installed, starting with coupled spiral and split-ring resonators. Properties of these resonators and the status of the project are discussed.

## Introduction

Significant upgrading of static accelerators can be obtained only by post-acceleration. For this purpose independently-phased short rf cavities are well suited. Normal conducting spiral and split-ring resonators combine high-shunt impedance with flexibility over a wide range of particle energies. Modular design and ease of fabrication are other important arguments for these structures to be used in relatively small post-accelerator projects. Our work concentrated on theoretical and experimental optimization of spiral and split-ring resonators for high field levels at good mechanical and electrical stability.

This post-accelerator project was funded in late 1978 with a budget of 0.4 MDM. Two accelerator sections and a buncher-chopper system will be installed at the 7-MV Van de Graaff generator at the Institut für Kernphysik in Frankfurt.[1,2] The improvement of the Van de Graaff generator, including the development of a new Penning ion source, cooling and power supply is being done by the Institut für Kernphysik.

## Layout of the Post-Accelerator

A schematic representation of the accelerator is shown in Fig. 1. The beam transport and the accelerator system have been designed to fit into the existing experimental area. The beam from the Van de Graaff passes a foil stripper, is then bent horizontally, and after bunching, chopping, and accelerating is bent back to the ground floor, where a new experimental area will be installed. Beam matching and radial focusing is obtained by two triplets and a quadrupole doublet. The design of the machine is to reach a voltage gain of 1 MV per accelerator section, which leads to the ion energies summarized in Table 1. Ions between N and Ar will be accelerated to energies between 1 and 2 MeV/N at an estimated particle current between 5 and 20 nA. A future plan is to place the stripper at 4.1 MV in the accelerator tube,[1] which will give another increase in particle energy, but presents problems with respect to service and damage of the accelerator tube.

The limiting factor in a post-accelerator project like this is the cost of the transmitters. An existing rf transmitter was rebuilt which yields up to 100-kW in pulsed as well as in cw operation. A second transmitter with 80-kW pulsed power is of the same type as used in the Heidelberg post-accelerator project and will be delivered in November.

The buncher amplifier, the transistorized preamplifiers, and the regulation and control system are developed and built by ourselves. The control system consists of three parts: a slow resonance frequency control tuning capacity, a fast amplitude control, which keeps the amplitude constant within 0.5%, and a fast phase control, which gives a phase ripple of less than 1°. First tests have shown that the design values can be obtained. In this stage of the project, no computer control

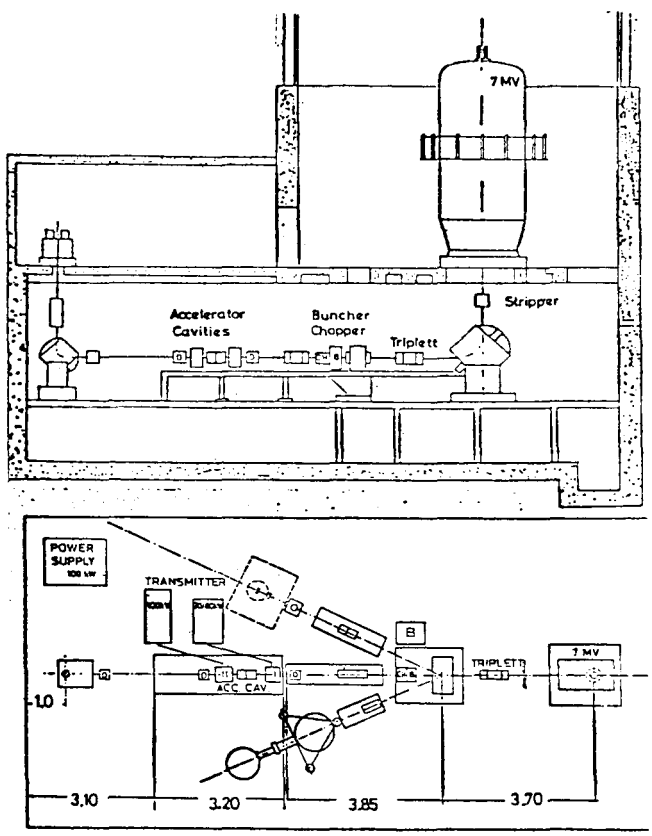


Fig. 1 Layout of the accelerator system

* Work supported by BMFT and DFG.

is planned because the system is rather simple. Later, microcomputers may support manual operation.

| PROJECTILE | $z_A$ | z | $E_0$ CN-OUTPUT [MeV] | $E_0$ CN-OUTPUT [MeV/N] | $E_1$ [MeV/N] | $E_2$ [MeV/N] | $E_2$ [MeV] |
|---|---|---|---|---|---|---|---|
| $^{14}_{7}N$ | 2 | 6 | 14 | 1.0 | 1.43 | 1.86 | 26.0 |
| $^{20}_{10}Ne$ | 3 | 8 | 21 | 1.05 | 1.45 | 1.85 | 37.0 |
| $^{27}_{13}Al$ | 3 | 8 | 21 | 0.78 | 1.1 | 1.4 | 37.8 |
| $^{32}_{16}S$ | 3 | 9 | 21 | 0.66 | 0.90 | 1.15 | 36.8 |
| $^{40}_{18}Ar$ | 4 | 10 | 28 | 0.7 | 1.06 | 1.42 | 56.8 |

$5\ nA \leq I_{outp.} \leq 20\ nA$

Table 1 Ion energies of the accelerator system

## Accelerator Structures

The post-accelerator will partly be used as a test facility for the development of new accelerator structures. So even at the first stage two different structures will be used. The spiral structure, which will be discussed first, is well developed and tested.[3-9]

For this project a further development using electromagnetically-coupled spirals was tried, to increase the efficiency. Thus, the rather high design value of 1-MV resonator was obtained with our transmitters (80 - 100 kW, 25% dc).

The spiral resonator is a two-gap structure with the spiral conductor excited to quarter wavelength oscillations (Fig. 2):

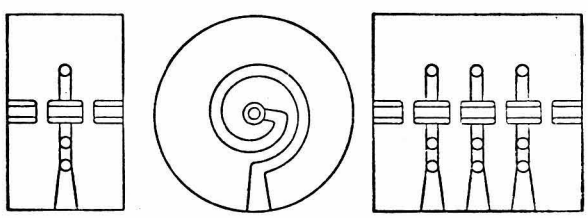

Fig. 2 Schematic drawing of the spiral resonator

Optimization shows that the efficiency, which is characterized by the shunt impedance $\eta$,

$$\eta = \frac{E_{acc}^2}{N/L} = \frac{\Delta U^2}{N \cdot L}$$

$$\Delta U = \int_0^L E(z)\cos(\omega t - \phi)\,dz$$

($\Delta U$ voltage gain, $E_{acc}$ average accelerating field, L cavity length, N rf power.)

decreases with increasing spiral tube diameter, caused by increased capacitive load. On the other hand, for good mechanical stability, a large tube diameter would be best. It becomes obvious that maximum efficiency and maximum stability exclude each other. With the single spiral prototypes, effective accelerating fields up to 6 MV/m and voltage gains up to 1.3 MV per resonator, have been achieved for pulse power of 200-kW, with excellent stability. An even smaller value of $\Delta f_{stat}$ = 0.05 Hz/kW was obtained with a single spiral buncher cavity, which was built for the Unilac. A single spiral resonator with a tube diameter of 15 mm and an $\eta$ of 42 MΩ/m, will be used as the buncher cavity. A significant increase in efficiency is obtained by combining several electro-magnetically-coupled spirals in one cavity, as shown in Fig. 2. For the case in which the properties of the individual spiral remain unchanged and the rf power per cavity is constant, the voltage gain $\Delta U$ of such a resonator increases with the square root of the number of spirals

$$\Delta U_n = \sqrt{n} \cdot E_{acc} \cdot L \quad .$$

The $R_p$ value, defined as $\eta$ times length L of the cavity,

$$R_p = \eta \cdot L = \frac{\Delta U^2}{N} = n \cdot \frac{\Delta U_0^2}{N}$$

is proportional to n, the number of spirals. This increase in efficiency; however, leads to some reduction of flexibility with increasing number of spirals per cavity. This is demonstrated in Fig. 3, which shows transit time curves for cavities with different numbers of spirals. Resonators with 3 electro-magnetically-coupled spirals were chosen as a good compromise. Resonators with coupled spirals have several modes of oscillation. The so-called $\pi$-mode, where adjacent spiral drift tubes have opposite polarity, has in all realistic cases the highest shunt impedance and the lowest resonance frequency. The frequency, the parameters of the spirals, and the distribution of the fields in the resonator depend strongly on the coupling mode and strength. A lot of work has been done to ensure equal distribution of rf power to the different spirals. This flatness is necessary to minimize static frequency shift in order to get high stability of the resonator.

At design field levels, forces cannot be neglected, and any structure may be stimulated to mechanical vibrations.[6] Forces of up to 2 kp tend to detune the spiral conductors. Mechanical displacement of the drift tube up to several mm, corresponding to a frequency shift of $\Delta\nu \approx 1$ MHz, have been observed. This has been measured with cavities specially designed to study these ponderomotive effects. High power measurements of such resonators with coupled spirals, indicated that all the axial fields should also have the same value to compensate the axial forces. This is done by using approximately a half gap-length

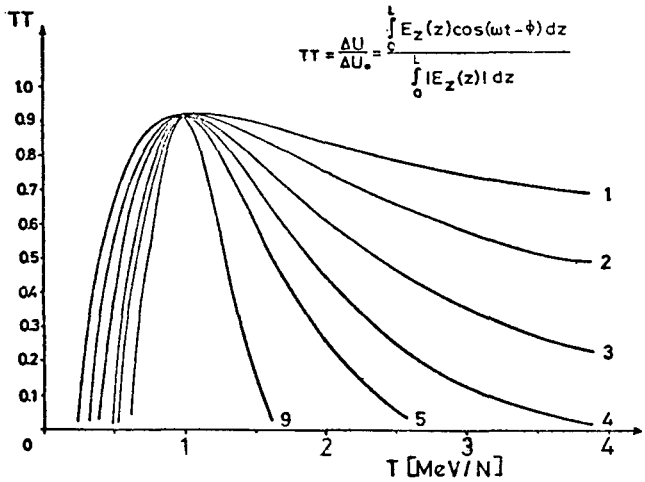


Fig. 3 Transit time factor TT as function of particle energy T.
Parameter: number of spirals per cavity

between spirals and end plates, a "flat" field distribution. Equal distribution of rf power to the individual spirals can be reached by choosing the resonance frequency of the "end spirals" lower than for the central one. The ratio of resonance frequencies depends on coupling strength between the spirals, which is usually very high. The coupling can be described in terms of the frequency separation of π-mode and 0-mode, which can be as high as 65 MHz with a π-mode of 108.5 MHz. Such strong coupling is obtained by arranging the spirals to alternate the winding direction, thus adding capacitive and inductive coupling. The frequency-tuning of the individual spirals is done by varying the length of the spiral tube, which in some cases differs up to 30%. Additionally, the coupling of the spirals leads to a further field concentration near the axis, and gives a better shunt impedance. η values of 47 MΩ/m were measured, compared with only 25 MΩ/m for single spirals with the same parameters.

The first cavity of the post-accelerator is a three-spiral resonator optimized for a particle energy of 1 MeV/N (Table 2).

Tank length 32 cm,
Tank diameter 35 cm,
Spiral tube diameter 20 mm,
Drift tube diameter 40 mm,
Drift tube length 50 mm,
Aperture diameter 20 mm,
Gap length 20 mm, end plate gap 9 mm,
Resonance frequency 108.5 MHz, Q = 4200,
$\eta_o$ = 55 MΩ/m, $\eta_{eff}$ = 45.5 MΩ/m, $R_{P_{eff}}$ = 14.6 MΩ,
$T_o$ = 1 MeV/N, ΔU (100 kW) = 1.2 MV,
$E_{acc}$ (100 kW) = 3.8 MV/m

Table 2 Parameters of the 3-spiral resonator

The individual spirals have been milled out of copper plates and brazed together as indicated in Figure 4. Additionally, the spirals and the

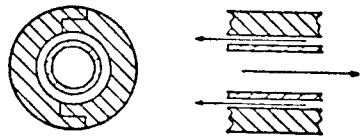

Fig. 4 Cross-section of the spiral tubing

water-cooled drift tubes had been copper-plated and placed in a copper-plated stainless steel tank (L = 32 cm, diameter 35 cm). The parameters of the spirals and the coupling strength can be calculated approximately. The final tuning is done by iteratively mapping the field and changing the resonance frequencies of the individual spirals. Figure 5 shows the final axial accelerating field of the first post-accelerator cavity, which has a shunt impedance of 45 MΩ/m.

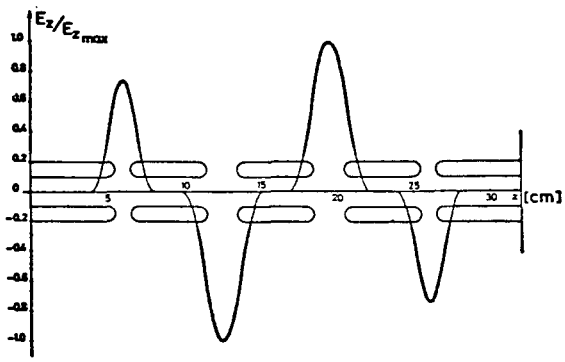


Fig. 5 Axial field distribution of the 3-spiral resonator

In Figure 6, the transit time factor is plotted versus the particle energy. Figure 7 shows a view of this first post-accelerator cavity. In high power tests with this spiral resonator, a voltage gain of ΔU = 1.2 MV was obtained for an rf power of 100 kW in pulsed operation. This corresponds to an accelerating field of 3.8 MV/m.

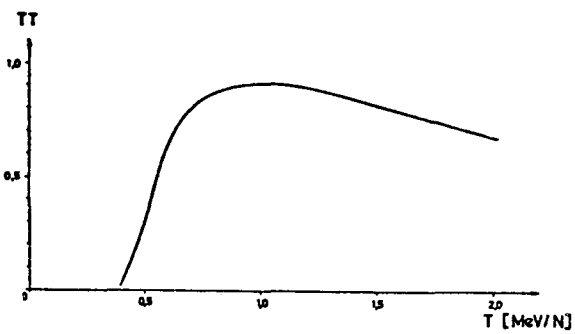


Fig. 6 Transit time factor TT as function of the particle energy T for the spiral resonator

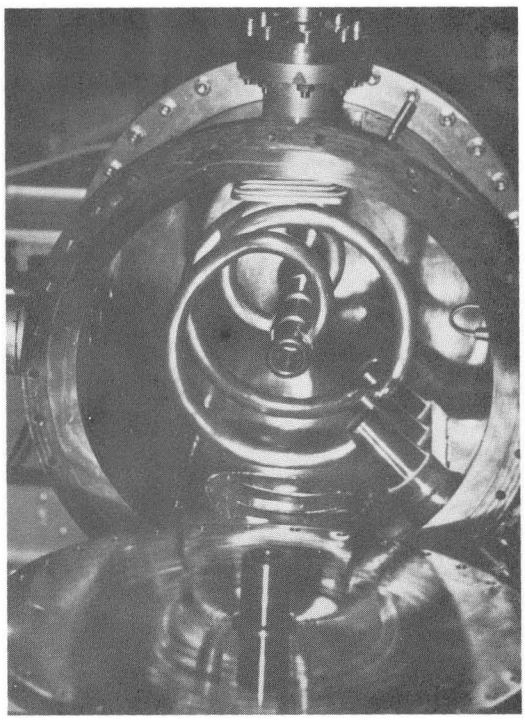

Fig. 7 View of the 3-spiral resonator

The second structure to be used in the project is the split ring. The split-ring resonator was first proposed at CIT and is used as a superconducting post-accelerator structure in the Argonne and Stony Brook tandem boosters.[10-12] We have done work on normal conducting split-ring versions since 1976. The optimization of split-ring resonators with respect to a high shunt impedance and good mechanical stability, leads to similar results for the geometrical shape as in the superconducting case.

Figure 8 shows a schematic drawing of this structure. It consists of two coupled $\lambda/4$ resonators shaped like two "semi-rings" and ending in drift tubes, which oscillate with 180° phase difference. This arrangement may be compared with two coupled spirals with rather large pitch, mounted on a common "leg". For high efficiency, in this case, a slightly larger tank is needed to reduce the capacitive load compared with separate spiral resonators. Values for the shunt impedance

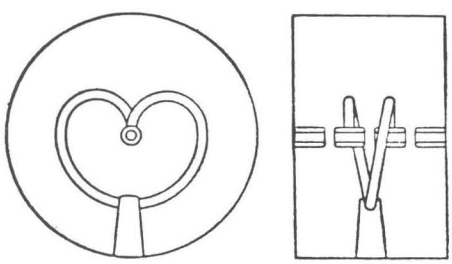

Fig. 8 Schematic drawing of the split-ring resonator

$\eta$ up to 60 MΩ/m and voltage gains of 1 MV/resonator[13] have been achieved with prototype units. The detuning due to radiation pressure, which is represented by the static frequency shift, is comparable to that of a spiral resonator, ranging from 0.2 to 5 kHz/kW.

Table 3 shows the parameters of the split-ring resonators, and in the last row, the parameters of the second post-accelerator split-ring cavity, which is optimized for a particle energy of 1.3 MeV/N.

| TANK LENGTH [mm] | TANK DIAM. [mm] | SPLITRING TUBE DIAM. [mm] | DRIFT TUBE DIAM. [mm] | GAP WIDTH [mm] | $Q_0$ | $\eta_{EFF}$ [MΩ/m] | $R_{P_{EFF}}$ [MΩ] | RF POWER [kW] | $\Delta W_{EFF}$ [MV] | $E_{Z_{EFF}}$ [MV/m] |
|---|---|---|---|---|---|---|---|---|---|---|
| 181 | 350 | 18 | 4 | 15 | 4300 | 38.6 | 7.0 | 70 | 0.7 | 3.9 |
| 208 | 350 | 18 | 6 | 20 | 4120 | 29.1 | 7.0 | 100 | 0.84 | 4.0 |
| 240 | 350 | 18 | 4 | 28 | 3900 | 34.8 | 7.2 | 125 | 0.95 | 3.9 |
| 290 | 500 | 22 | 4 | 20 | 5400 | 59.6 | 17.3 | (80) | (1.18) | (4.1) |

Table 3 Parameters of split-ring resonators

The axial field distribution and the transit time factor TT are plotted in Figures 9 and 10.

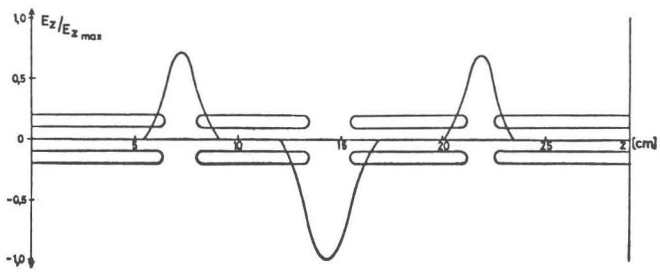


Fig. 9 Axial field distribution of the split-ring resonator

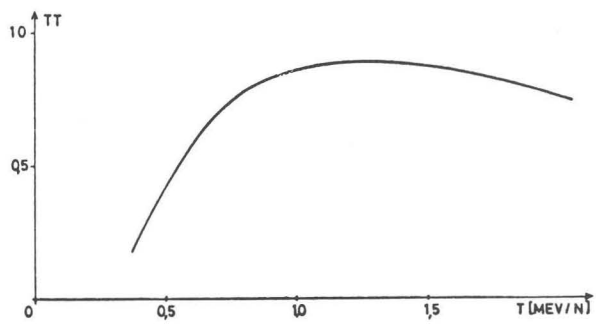


Fig. 10 Transit time factor TT as function of particle energy for the split-ring resonator

Figure 11 shows a view of this normal conducting split-ring resonator, which will undergo

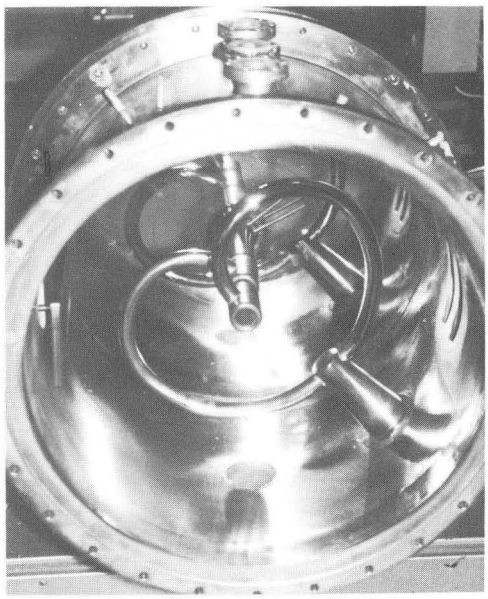

Fig. 11 View of the split-ring resonator

rf tests at the end of September.

## Beam Dynamics

The post-accelerator will have a normalized acceptance of 3π cm-mrad. The calculations have been done with a code including non-linear coupling between radial and axial phase space. The emittance of the Van de Graaff will be matched with two triplets to give a circular beam envelope at the entrance of the post-accelerator, with gradients between 0.5 and 1.5 kG/cm, and 2 cm aperture diameter. Energy resolution of the heavy ion beam will be between $10^{-3}$ and $10^{-2}$. Pulse lengths of 0.4 nsec can easily be produced depending upon tuning of the buncher-chopper system. Thus the beam emittance will be increased by a factor of about 4, which is reducable with help of a debuncher-rebuncher system.

## Status

The first accelerator cavity, the 3 coupled-spirals module, together with the 100-kW transmitter, the control system, the cooling and the power supply are completed and have been tested. High power tests of the split-ring resonator will start in September. In October the sections, the first transmitter, and the buncher-chopper system will be installed at the Van de Graaff generator, and first beam tests can be done. After delivery of the second rf transmitter in November, the post-accelerator will be completed, so that an improved heavy ion beam will be available at the beginning of next year.

Future plans include the insertion of new accelerator structures, such as rf quadrupole cavities, and modified IH resonators using the pc t-accelerator as beam test facility.

## Acknowledgements

The authors would like to express their gratitude to K. Meinel (Institut für Kernphysik), H. Stöcker, W. Blum, and K. Küllenberg (Institut für Angewandte Physik).

## References

1 K. Bethge, H. Baumann, K. Meinel, H. Klein, P. Junior, A. Schempp, H. Deitinghoff, Proc. 4th Conf. Appl. Small Acc., Denton 1976.

2 A. Schempp, Int. Rep. 78-11, 1978.

3 G.J. Dick, K.W. Shephard, Appl. Phys. Lett. 24 (1974) 40.

4 D.D. Armstrong et al., LA-UR 74-211 and Part. Acc. 6 (1975) 175.

5 A. Schempp, H. Klein, Nucl. Instr. Meth. 135 (1976) 409.

6 A. Schempp, W. Rohrbach, H. Klein, Nucl. Instr. Meth. 140 (1977) 1.

7 A. Schempp, H. Klein, Proc. 1976 Proton Linear Acc. Conf., Chalk River 1976, AECL-5677 (1977) 67.

8 E. Jaeschke, H. Ingwersen, R. Repnow, Th. Walcher, B. Huck, B. Kolb, Nucl. Instr. Meth. 157 (1978) 195.

9 E. Jaeschke, H. Ingwersen, R. Repnow, Th. Walcher, B. Huck, B. Kolb, IEEE Trans. NS-26 (1979) 3667, Proc. 1979 Part. Acc. Conf., San Francisco 1979.

10 K.W. Shephard, J.E. Mercereau, G.J. Dick, IEEE Trans. Nucl. Sci. NS-22 (1975) 1979.

11 K.W. Shephard, IEEE Trans. Nucl. Sci. NS-26 (1979) 3659, Proc. 1979 Part. Acc. Conf., San Francisco 1979.

12 J.R. Delayen, G.J. Dick, J.E. Mercereau, J.W. Noe, P. Paul, G.D. Sprouse, IEEE Trans. Nucl. Sci. NS-26 (1979) 3664, Proc. 1979 Part. Acc. Conf., San Francisco 1979.

13 E. Muller, G. Lotterbach, A. Schempp, Int. Rep. 78-5, 1978.